RESEARCH ARTICLE
doi: 10.2306/scienceasia1513-1874.2026.049

ScienceAsia 52 (3): 2026: ID 2026049: **1–8**

Glyphosate detection by specific inhibition of the nanozyme activity of MOF-808-NH_2: A dual-mode sensor with enhanced reliability for analysis

Chuhan Bian

School of Chemical Engineering and Technology of Tiangong University, Tianjin 300387 China

e-mail: 2411510215@tiangong.edu.cn

Received 24 Nov 2025, Accepted 7 May 2026
Available online 29 May 2026

ABSTRACT: This study successfully constructed an efficient colorimetric/fluorometric dual-mode nanozyme sensor based on a metal-organic framework (MOF-808-NH_2) for the highly selective and sensitive detection of glyphosate (GP). The sensor leverages the dual functionalities of MOF-808-NH_2, namely its intrinsic peroxidase-like activity and blue fluorescence emission. In the presence of hydrogen peroxide (H_2O_2), MOF-808-NH_2 catalyzes the oxidation of colorless 3,3′,5,5′-tetramethylbenzidine (TMB) to generate blue oxTMB, producing a distinct colorimetric signal. Simultaneously, the generated oxTMB quenches the inherent blue fluorescence of MOF-808-NH_2 via the inner filter effect (IFE). GP specifically inhibits the peroxidase-like activity of MOF-808-NH_2, leading to a reduction in oxTMB generation. This inhibition results in a dual-mode response: a weakening of the blue color (decreased colorimetric signal) and a recovery of the blue fluorescence (enhanced fluorescence signal). This dual-signal response strategy effectively integrates the intuitiveness of colorimetric analysis with the high sensitivity of fluorescence detection, eliminating the need for unstable biological enzymes, demonstrating good reliability, accuracy, and broad application prospects in the analysis of real samples. It provides a core driving force for achieving comprehensive connectivity between precision agriculture and environmental health.

KEYWORDS: metal-organic frameworks, dual-mode sensing, glyphosate detection, environmental safety

INTRODUCTION

GP is a broad-spectrum, non-selective, systemic amino acid herbicide. Owing to its simple synthesis, low cost, and high efficacy, it has been extensively used worldwide for effective weed control and enhancing crop yields [1]. However, GP and its primary metabolite, aminomethylphosphonic acid (AMPA), have been widely detected in soil and water bodies. Although their half-lives are not particularly long, persistent use has rendered them environmental background contaminants [2]. Currently, various analytical methods have been developed for the detoxification or detection of GP. Although laboratory chromatographic techniques offer high sensitivity and selectivity for GP, they are often costly and time-consuming [3, 4]. Furthermore, most colorimetric and fluorescence sensors relying on enzyme-based detection—such as organophosphorus hydrolase (OPH)—are limited in practical application due to enzyme instability and high cost [3, 5]. Therefore, there is a significant demand for the development of cost-effective, efficient, and reliable alternative analytical methods for detecting GP residue levels in the fields of environmental monitoring and food safety analysis.

Over the past decade, MOFs have emerged as a novel class of nanomaterials demonstrating significant potential in environmental remediation and monitoring [6]. Their highly designable pore structures, exceptionally high specific surface areas, and the strong Lewis acidity of their metal nodes enable MOFs to function as efficient bio-inspired materials [7]. They can rapidly hydrolyze organophosphorus compounds (such as pesticides and nerve agents) by activating the phosphoester bonds, effectively reducing their toxicity [8, 9]. The 2025 Nobel Prize in Chemistry was awarded to Susumu Kitagawa, Richard Robson, and Omar M. Yaghi in recognition of their pioneering contributions to the development of MOFs materials. The foundational properties they established—high surface area, tunable porosity, and customizable functionality—further underscore the broad prospects of MOFs for precise pollution prevention and control, as well as the highly efficient degradation of toxic substances [10]. Meanwhile, given that GP is an organophosphorus compound, integrating it with MOFs to design a dual-mode detection method presents a promising strategy for achieving rapid, reliable, cost-effective, convenient, and highly sensitive detection of GP.

In this study, an efficient colorimetric/fluorometric dual-mode nanozyme sensor was constructed by designing a GP-responsive MOFs catalytic system (Fig. 1). First, the nanomaterial MOF-808-NH_2, which possesses blue fluorescence emission characteristics and peroxidase-like activity, was prepared. In the presence of H_2O_2, MOF-808-NH_2, by virtue of its peroxidase-like activity, decomposes H_2O_2 into •OH radicals, which

subsequently catalyze the oxidation of colorless TMB to generate blue oxTMB [11]. Due to the IFE between the generated oxTMB and MOF-808-NH_2, the blue fluorescence of MOF-808-NH_2 is effectively quenched. The selective inhibition of the MOF material's peroxidase-like activity by GP impedes the TMB oxidation reaction, resulting in a decrease in oxTMB generation as the GP concentration increases. This inhibition consequently leads to a dual-mode response characterized by a weakened colorimetric signal and a recovered fluorescence signal [12, 13]. This dual-mode sensing strategy integrates the intuitiveness of colorimetric analysis with the high sensitivity of fluorescence detection. The complementary signals effectively overcome the limitations of single-mode analysis, significantly enhancing the reliability and accuracy of the assay [14]. It provides a novel technological pathway for the rapid, cost-effective, and efficient monitoring of GP residues in the environment, holding significant value for safeguarding environmental safety.

MATERIALS AND METHODS

Reagents and apparatus

H_3BTC (Trimesic acid), polyphenols, glutamic acid, cysteine, glutathione, glucose (D-glucose), thiamethoxam, glyphosate, chlorothalonil, diazinon, and $ZrOCl_2 \cdot 8\,H_2O$ (Zirconyl chloride octahydrate) were purchased from Sinopharm Chemical Reagent Co., Ltd. (Shanghai, China). Hydrogen peroxide (H_2O_2), 3,3′,5,5′-tetramethylbenzidine (TMB), DMF (N,N-dimethylformamide), H_2BDC-NH_2 (2-aminoterephthalic acid), formic acid, and acetone were obtained from MacLean Biochemical Technology Co., Ltd. (Shanghai, China). All reagents used throughout the experiment were analytical grade without further purification, and water used was the ultrapure water.

The UV-Vis absorption spectra were recorded using a TU-1901 UV-Vis spectrophotometer (PERSEE, Beijing, China). All fluorescence emission spectra were collected with a PerkinElmer LS-55 fluorescence spectrometer (PerkinElmer, Shanghai, China). X-ray diffraction (XRD) analysis of MOF-808-NH_2 was performed using a Rigaku D/MAX2500VL/PC X-ray diffractometer (Thermo Fisher Scientific, USA). Transmission electron microscopy (TEM) images of MOF-808-NH_2 (supported on a copper grid) were obtained using a JEM-2100 transmission electron microscope (JEOL Ltd., Japan). X-ray photoelectron spectroscopy (XPS) of MOF-808-NH_2 was conducted with an ESCALAB 250Xi X-ray photoelectron spectrometer (Thermo Electron, USA). The Fourier transform infrared (FT-IR) spectrum was obtained using a Bruker TENSOR 27 spectrometer. Zeta potential analysis of MOF-808 and MOF-808-NH_2 was performed using a Zetasizer (Nano-ZSE, Malvern, UK).

Synthesis of MOF-808-NH_2

MOF-808-NH_2 was synthesized according to a previously reported method with modifications [15]. Typically, H_3BTC (0.1175 g), H_2BDC-NH_2 (0.1014 g), and $ZrOCl_2 \cdot 8\,H_2O$ (0.54 g) were dispersed in 30 ml of a mixed solvent of DMF and formic acid (v/v = 1:1). The mixture was ultrasonicated for 15 min and then transferred into a Teflon-lined autoclave, which was heated at 120 °C for 48 h. After cooling to room temperature naturally, the resulting solid was collected and washed three times with DMF and acetone via centrifugation at 9,000×g. The final product was dried at 60 °C for 6 h to yield MOF-808-NH_2.

Evaluation of the catalytic activity of MOF-808-NH_2

The catalytic performance of MOF-808-NH_2 was evaluated using H_2O_2 as the substrate and TMB as the chromogenic agent. The experimental procedure was as follows: six reaction systems were prepared containing 50 µg/ml MOF-808-NH_2 + 200 µM H_2O_2; 50 µg/ml MOF-808-NH_2 + 1 mM TMB; 1 mM TMB; 200 µM H_2O_2; 200 µM H_2O_2 + 1 mM TMB; and 50 µg/ml MOF-808-NH_2 + 200 µM H_2O_2 + 1 mM TMB, respectively. Each mixture was diluted to a final volume of 200 µl with 5 mM sodium acetate-acetic acid (HAc-NaAc) buffer (pH = 4), thoroughly mixed, and then reacted in a metal bath at 45 °C for 15 min. The color change of the solution was observed, and the absorbance at 652 nm was measured.

Steady-state kinetic assays were performed in HAc-NaAc buffer (5 mM, pH 4) containing 50 µg/ml MOF-808-NH_2. The concentration of TMB (0–1 mM) or H_2O_2 (0–20 mM) was varied individually while keeping the concentration of other components constant. Double-reciprocal plots of reaction velocity versus TMB or H_2O_2 concentration were calculated using the Michaelis-Menten equation (Eq. (1)):

$$\frac{1}{V} = \frac{K_m}{V_{\max}[S]} + \frac{1}{V_{\max}} \tag{1}$$

where $[S]$ is the concentration of substrate, K_m is the Michaels constant, V is the reaction rate, and $V_{\max}$ is the maximum reaction rate.

Development of a MOF-808-NH_2-based dual-mode sensor for GP detection

First, GP was prepared at different concentrations from 0 to 250 µM. Subsequently, 200 µM H_2O_2, 50 µg/ml MOF-808-NH_2, and 1 mM TMB were mixed with different concentrations of GP and allowed to react completely in a 5 mM HAc-NaAc buffer (pH = 4) at 45 °C. After 15 min, the reaction solutions were taken for analysis using a TU-1901 UV-visible spectrophotometer and a PerkinElmer LS-55 fluorescence spectrophotometer, respectively.

To validate the specificity, a mixture containing 200 µM H_2O_2, 50 µg/ml MOF-808-NH_2, and 1 mM

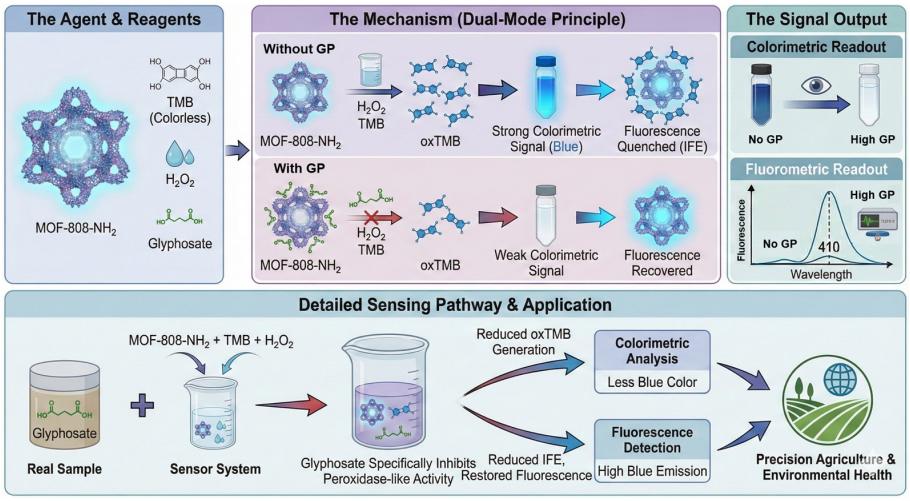

Fig. 1 Schematic of a novel colorimetric and fluorescent dual-mode nanozyme sensor for GP detection based on the nanozyme MOF-808-NH_2.

TMB was separately mixed with Pb^{2+}, Cu^{2+}, Mg^{2+}, Cl^-, I^-, tea polyphenols, glutamate, cysteine, glutathione, glucose, thiamethoxam, furosemide, chlorothalonil, trichlorfon, and tetramethrin. The reactions were carried out in a 5 mM HAc-NaAc buffer (pH = 4) at 45 °C for 15 min, followed by colorimetric and fluorescence analyses.

Dual-mode detection of glyphosate in real samples

To evaluate the detection performance of the system for GP in real samples, tea leaves, tobacco and cabbage were selected as the real-world matrix in this study. The real samples were collected from randomly selected farm fields. Sample pretreatment was carried out according to a literature method with minor modifications [16]. Briefly, the samples were ground into a fine powder and thoroughly homogenized. Then, 1 g of the powdered sample was transferred into a centrifuge tube and sonicated with 3 ml of deionized water for 3 min. The mixture was subsequently centrifuged at 1,400×g for 2 min, and the supernatant was collected as the sample extract. The extract was spiked with GP at concentrations of 0, 10, and 20 µM, respectively. Thereafter, all samples were reacted with 200 µM H_2O_2, 50 µg/ml MOF-808-NH_2, and 1 mM TMB in 5 mM HAc-NaAc buffer (pH = 4) at 45 °C for 15 min. Finally, the samples were analyzed using two detection modes.

RESULTS AND DISCUSSION

Synthesis and characterization of MOF-808-NH_2

MOF-808-NH_2 was synthesized via a solvothermal method, employing H_3BTC or H_2BTC-NH_2 as auxiliary ligands to compete for coordination with the Zr_6 cluster [17]. The TEM image indicates that the synthesized MOF-808-NH_2 exhibits an octahedral morphology (Fig. 2A,B). Meanwhile, energy-dispersive X-ray spectroscopy (EDS) elemental imaging analysis indicates that the material primarily C, N, Zr (Fig. 2C–F). The obtained samples exhibited XRD reflections matching the simulated pattern derived from the MOF-808 single crystal, confirming crystallinity (Fig. S1). The FT-IR spectrum confirms the characteristic bidentate coordination of Zr^{4+} with carboxylate groups in the MOF-808 structure, evidenced by the absence of a free carboxyl band (1730–1710 cm^{-1}) and the presence of distinctive Zr(μ_3)–O vibrations at 645 and 756 cm^{-1} (Fig. S2) [18]. XPS was used to further investigate the chemical states of elements in the as-prepared MOFs, and the findings regarding elemental presence agreed well with the EDS results (Fig. S3). It is noteworthy that MOF-808-NH_2 exhibits maximum fluorescence emission intensity at an excitation wavelength of 325 nm (Fig. S4).

Study on the peroxidase-like activity of MOF-808-NH_2

Utilizing TMB as a probe, the peroxidase-like activity of the synthesized MOF-808-NH_2 was investigated. The oxidation of TMB, catalyzed by the material in the presence of reactive oxygen species (ROS), yields a characteristic blue product (oxTMB), resulting in a measurable increase in absorbance at 652 nm. The study revealed that only the mixture of MOF-808-NH_2, H_2O_2, and TMB developed a distinct blue color and exhibited a significant enhancement in absorbance at 652 nm, whereas the other control systems showed almost no change in both color and absorbance (Fig. 3A,B). It can be concluded that MOF-808-NH_2 exhibits peroxidase-like activity. It catalyzes the decomposition of H_2O_2 to generate ROS, specifically hydroxyl radicals (•OH).

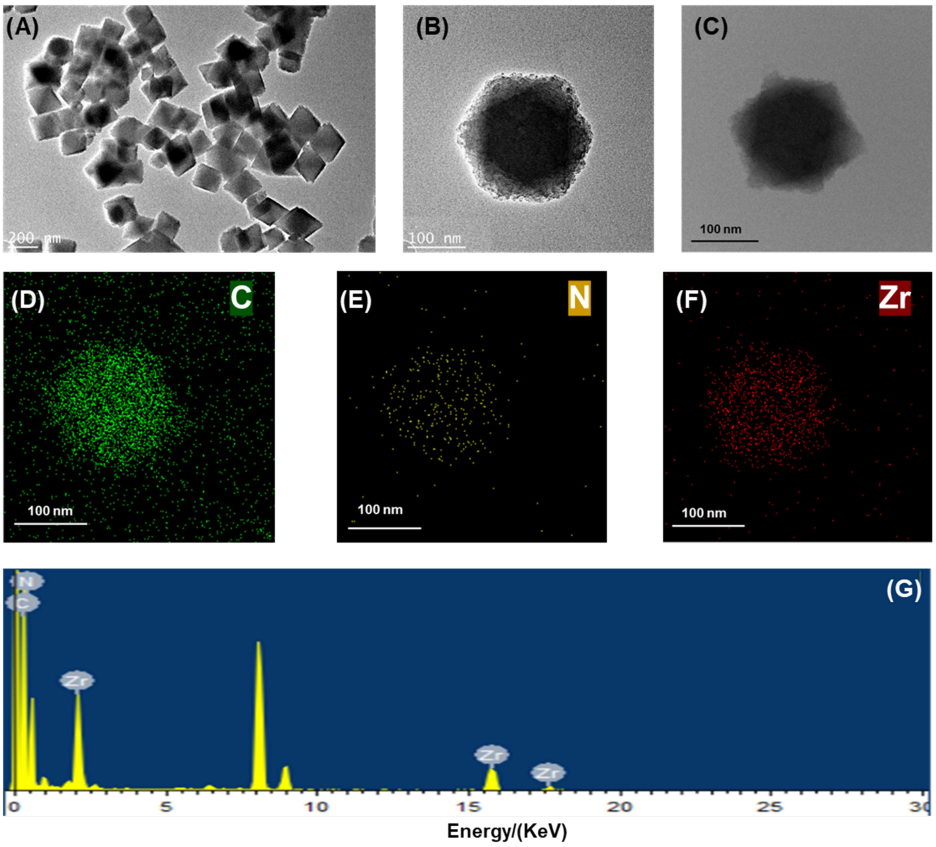

Fig. 2 (A, B) TEM images of MOF-808-NH_2, (C) STEM image, and (D, E, F) elemental mapping of C, N, Zr, respectively. (H) EDS spectrum of MOF-808-NH_2 (the support film is a copper lattice).

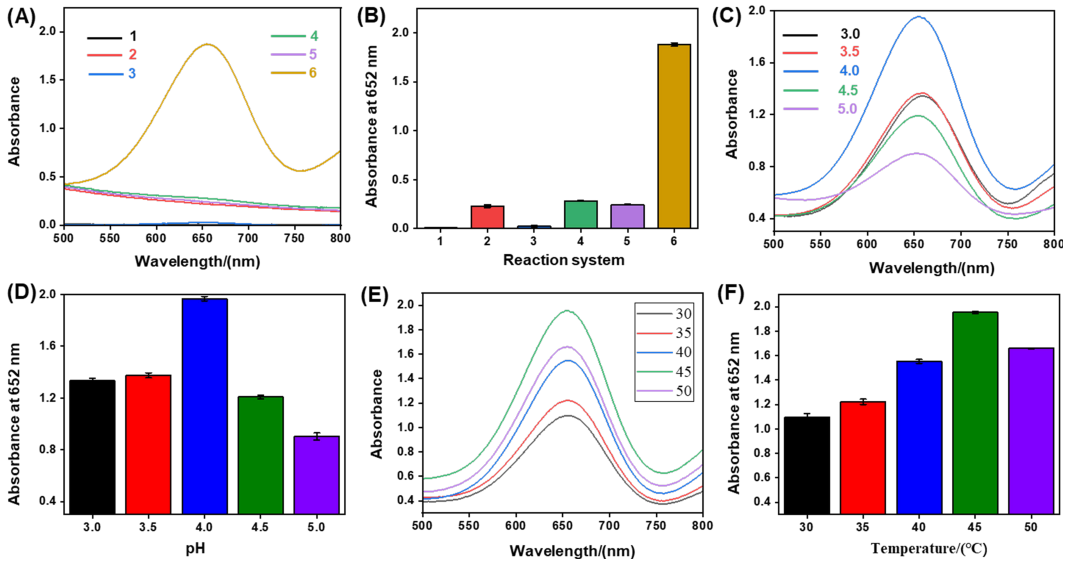

Fig. 3 (A) Absorption spectra of (1) MOF-808-NH_2 + H_2O_2, (2) MOF-808-NH_2 + TMB, (3) TMB, (4) H_2O_2, (5) H_2O_2 + TMB, and (6) MOF-808-NH_2 + H_2O_2 + TMB. (B) Absorbance at 652 nm was compared for different reaction systems as shown in (A). Effects of (C) pH and (E) temperature on the MOF-808-NH_2 + H_2O_2 + TMB system. (D, F) Absorbance at 652 nm was compared for different reaction systems as shown in (C) and (E). Experimental conditions: MOF-808-NH_2, 50 µg/ml; H_2O_2, 200 µM; TMB, 1 mM; HAc-NaAc buffer (pH = 4); 15 min; 45 °C.

These •OH radicals subsequently oxidize the colorless chromogenic substrate TMB to form deep blue oxTMB, resulting in a significant increase in absorbance at 652 nm [19, 20]. It was found that the Michaelis–Menten constants (K_m) values of MOF-808-NH_2 were determined to be 0.324 mM for H_2O_2 and 0.219 mM for TMB. These K_m values are comparable to or even surpass that of native horseradish peroxidase [21], demonstrating that MOF-808-NH_2 possesses high affinity for its substrates and thus excellent catalytic efficiency (Fig. S5). The effects of pH and temperature on the peroxidase-mimicking activity of MOF-808-NH_2 were further investigated by monitoring the absorbance of TMB at 652 nm. The results indicated that the optimal pH and temperature for the activity of MOF-808-NH_2 were 4 (Fig. 3C,D) and 45 °C (Fig. 3E,F), respectively.

Development of a dual-mode colorimetric-fluorescence sensor based on GP-responsive MOF-808-NH_2 nanoenzymes

Based on the excellent peroxidase (POD)-like activity of MOF-808-NH_2, its application in the development of an effective analytical method for GP was further explored. It was found that GP could significantly inhibit the catalytic activity of MOF-808-NH_2. This inhibition is likely attributed to the binding of GP, which alters the substrate affinity of MOF-808-NH_2 and masks some of its POD-like active sites [22–24]. This leads to an interruption of the POD-like reaction and a reduction in •OH generation, consequently suppressing the oxidation of TMB to oxTMB. To verify this speculation, a gradual fading of the blue color was observed in the MOF-808-NH_2 + H_2O_2 + TMB system after reaction with GP (Fig. S6A). These results indicate that GP inhibits the POD-like activity of MOF-808-NH_2, thereby reducing the efficiency of TMB oxidation to oxTMB, which provides a basis for developing a colorimetric method for GP detection. Furthermore, due to the IFE of oxTMB on MOF-808-NH_2, the blue fluorescence of MOF-808-NH_2 at 410 nm was significantly quenched in the presence of TMB + H_2O_2 [25, 26]. However, the addition of GP suppressed the catalytic activity of MOF-808-NH_2 toward oxTMB generation, consequently blocking the IFE process and restoring the blue fluorescence emission of MOF-808-NH_2 (Fig. S6B). Based on the above analysis, it is feasible to construct a dual-mode detection system integrating both colorimetric and fluorescent signals for GP, leveraging its inhibitory effect on the POD-like activity of MOF-808-NH_2 in the presence of TMB and H_2O_2. Additionally, the optimal response time for GP in this system was determined to be 16 min, as both the GP-supplemented and GP-free MOF-808-NH_2 + H_2O_2 + TMB systems exhibited peak absorbance at 652 nm at this time point (Fig. 4A).

As shown in Fig. 4B,C, in the MOF-808-NH_2 + H_2O_2 + TMB system, a visible blue color fading was observed as the GP concentration increased, accompanied by a concentration-dependent decrease in absorbance at 652 nm. Furthermore, under 325 nm UV light irradiation (Fig. 4B,E), the same system exhibited a concentration-dependent enhancement of blue fluorescence brightness, along with a concurrent increase in fluorescence intensity at 410 nm. As illustrated in Fig. 4D,F, a linear relationship between the absorbance (A) and the GP concentration was established, yielding the equation $A = -0.00708x + 2.00487$ ($R^2 = 0.99705$), with a limit of detection (LOD) of 1.23 μM (LOD = $3\delta/k$, where δ is the standard deviation of 11 blank measurements and k is the slope of the calibration curve). Similarly, a linear relationship between the fluorescence intensity (F) and the GP concentration was obtained, described by $F = 7.80384x + 1664.81725$ ($R^2 = 0.99472$), with an LOD of 1.34 μM. The sensor showed a good linear relationship in the range of 1.23–230 μM for colorimetric mode and 1.34–230 μM for fluorescence mode. Compared with previously reported methods, the developed dual-mode nanozyme sensor not only exhibits competitive sensitivity, but also demonstrates significant comprehensive advantages in terms of providing a broader linear range, enabling visual on-site screening, and ensuring enzyme-free stability (Table 1). Based on these results, a dual-modal analytical platform integrating colorimetric and fluorescent signals was developed using MOF-808-NH_2 for the detection of GP. To evaluate the selectivity of the MOF-808-NH_2 + H_2O_2 + TMB dual-mode system for GP, several representative agrochemical substrates or common interferents—including Pb^{2+}, Cu^{2+}, Mg^{2+}, Cl^-, I^-, tea polyphenols, glutamate, cysteine, glutathione, glucose, thiamethoxam, furosemide, chlorothalonil, trichlorfon, and tetramethrin—were selected as reference substances. As illustrated in Fig. 5A,B, except for GP, none of the other tested substances induced noticeable colorimetric or fluorescent changes, indicating that the MOF-808-NH_2 + H_2O_2 + TMB system exhibits excellent selectivity toward GP. Furthermore, the anti-interference capability of the MOF-808-NH_2 + H_2O_2 + TMB system was investigated in the presence of the aforementioned coexisting species. The results demonstrated that each coexisting substance caused almost negligible variation in both the colorimetric and fluorescent signals induced by GP (Fig. 5C,D), suggesting that the dual-mode response of the MOF-808-NH_2 + H_2O_2 + TMB system is highly resistant to interference. This reinforces the potential of this platform for the reliable detection of GP residues in real samples.

Dual-mode nanozyme sensor for monitoring of GP in real samples

Subsequently, the practical utility of the proposed analytical platform for the dual-modal detection of GP in real agricultural products was evaluated. As shown

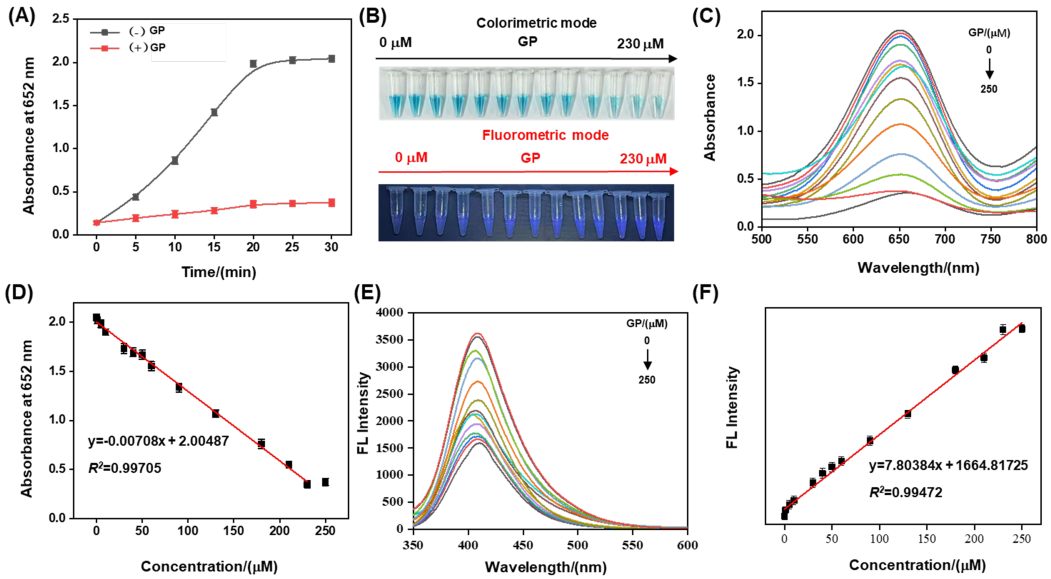

Fig. 4 (A) Time-dependent absorption intensities at 652 nm for MOF-808-NH_2 + H_2O_2 + TMB systems with (+) and without (−) GP. (B) Measurement of colorimetric and fluorescence image signals within the GP concentration range of 0–230 μM. (C) Absorption and (E) fluorescence spectra of MOF-808-NH_2 + H_2O_2 + TMB systems with different concentrations of GP in 0–250 μM. Calibration curve of (D) intensity of absorption spectra at 652 nm and (F) fluorescence intensity vs. GP concentration from 0–250 μM. Experimental conditions: MOF-808-NH_2, 50 μg/ml; H_2O_2, 200 μM; TMB, 1 mM; HAc-NaAc buffer (pH = 4); 20 min; 45 °C. Although concentrations up to 250 μM were tested, the linear response was maintained up to 230 μM.

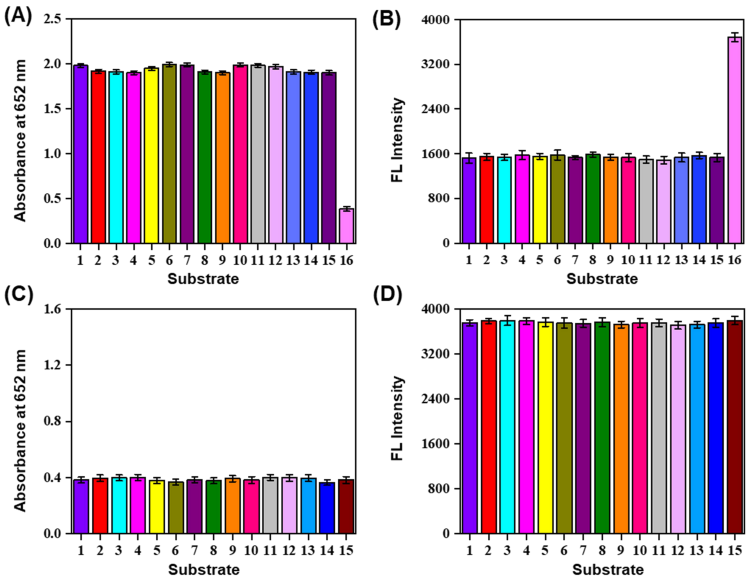

Fig. 5 Selectivity of (A) colorimetric and (B) fluorescence modes of MOF-808-NH_2 + H_2O_2 + TMB toward GP over other indicated substrates, including (1–16): Pb^{2+}, Cu^{2+}, Mg^{2+}, Cl^-, I^-, tea polyphenols, glutamate, cysteine, glutathione, glucose, thiamethoxam, furosemide, chlorothalonil, trichlorfon, tetramethrin and GP, respectively. Anti-interference testing of MOF-808-NH_2 + H_2O_2 + TMB system toward GP over other indicated interferences in (C) colorimetric and (D) fluorescence modes. (1–15): GP+ Pb^{2+}, Cu^{2+}, Mg^{2+}, Cl^-, I^-, tea polyphenols, glutamate, cysteine, glutathione, glucose, thiamethoxam, furosemide, chlorothalonil, trichlorfon and tetramethrin. Experimental conditions: MOF-808-NH_2, 50 μg/ml; H_2O_2, 200 μM; TMB, 1 mM; HAc-NaAc buffer (pH = 4); 20 min; 45 °C.

Table 1 Comparison of the analytical parameters of the MOF-808-NH_2 + H_2O_2 + TMB for GP detection with other reported methods.

Method	Material	Linear range (μM)	Detection limit (μM)	Ref.
Fluorescence	OPN-CD	0.3–6	/	[27]
Colorimetric	Cu_2^{II}-PV	0–4	2.66	[28]
UPLC-MS/MS	/	0.18–9.01	0.43	[29]
Colorimetric	CP-Cl	1–40	1.23	[30]
Photoelectrochemical	Au/ZnO/Co_3O_4/NF	100–900	100	[31]
Colorimetric & Fluorescence	MOF-808-NH_2	1.23–230 1.34–230	1.23 1.34	This work

/ means not applicable.

Table 2 A dual mode nanozyme sensor based on the MOF-808-NH_2 + H_2O_2 + TMB system combining colorimetric (C) and fluorescent (F) synergistic detection for GP detection in real samples.

Sample	Spiked (μM)	Detected (μM)		Recovery (%, $n = 3$)		R.S.D. (%, $n = 3$)		GC-MS (μM)
		C	F	C	F	C	F	–
Tea leaves	0	1.59	1.37	/	/	3.68	3.56	1.22
	10.00	11.66	11.58	100.70	102.10	4.05	4.14	11.14
	20.00	21.83	21.96	101.20	102.95	3.57	3.89	21.32
Tobacco	0	0.98	1.03	/	/	3.65	4.12	1.02
	10.00	10.99	10.82	100.10	97.90	2.76	0.86	10.37
	20.00	20.84	20.15	99.30	95.60	1.56	1.86	20.55
Cabbage	0	0.97	1.01	/	/	0.76	1.43	1.11
	10.00	10.54	10.85	95.70	98.40	1.64	2.45	11.24
	20.00	20.88	20.09	99.55	95.40	0.98	1.88	20.44

/ means not applicable.

in Table 2, the results obtained for GP in real agricultural samples using this dual-modal platform showed negligible differences compared to those acquired by the standard GC-MS method. Notably, the recovery rates ranged from 95.40% to 102.95%, with relative standard deviations (R.S.D.) of less than 5%. These results validate the significant potential of the proposed analytical platform for practical sample testing.

CONCLUSION

In summary, this study successfully constructed a novel colorimetric/fluorometric dual-mode nanozyme sensor for GP detection based on the nanozyme MOF-808-NH_2. The sensor operates on the principle that GP specifically inhibits the peroxidase-like activity of MOF-808-NH_2, thereby reducing the oxidation of TMB to oxTMB in the presence of H_2O_2. This inhibition generates two complementary signals: a decrease in colorimetric absorbance at 652 nm and a recovery of the material's inherent blue fluorescence at 410 nm due to the modulation of the IFE. The dual-signal output combines the intuitiveness of colorimetric analysis with the high sensitivity of fluorescence detection, effectively overcoming the limitations of single-mode sensors and significantly enhancing the reliability and accuracy of the assay. This work highlights the significant potential of functionalized MOFs in constructing reliable, enzyme-free sensing platforms. The proposed strategy not only provides a cost-effective and efficient tool for monitoring GP residues in environmental and agricultural samples but also opens up new avenues for the design of multi-modal sensing systems for other hazardous substances, contributing to the advancement of environmental safety and precision agriculture. Future research will focus on extending this platform to detect multiple contaminants simultaneously and developing portable devices for on-site analysis.

Appendix A. Supplementary data

Supplementary data associated with this article can be found at https://dx.doi.org/10.2306/scienceasia1513-1874.2026.049.

Acknowledgements: This research received no specific grant from any funding agency in the public, commercial, or not-for-profit sectors. No potential conflicts of interest relevant to this article were reported.

REFERENCES

1. Guo H, Wang H, Zheng J, Liu W, Zhong J, Zhao Q (2018) Sensitive and rapid determination of glyphosate, glufosinate, bialaphos and metabolites by UPLC-MS/MS using a modified Quick Polar Pesticides Extraction method. *Forensic Sci Int* **283**, 111–117.
2. Zou T, Jin C, Zhu Z, Hu Y (2019) Detection of glyphosate resistance in black nightshade *Solanum nigrum* from Hunan China. *ScienceAsia* **45**, 419–424.
3. Pundir C, Malik A, Preety (2019) Bio-sensing of organophosphorus pesticides: A review. *Biosens Bioelectron* **140**, 5–17.

4. Kaushal J, Khatri M, Arya S (2021) A treatise on organophosphate pesticide pollution: current strategies and advancements in their environmental degradation and elimination. *Ecotox Environ Safe* **207**, 111483.
5. Cai Y, Zhu H, Zhou W, Qiu Z, Chen C, Qileng A, Li K, Liu Y (2021) Capsulation of AuNCs with AIE effect into metal-organic framework for the marriage of a fluorescence and colorimetric biosensor to detect organophosphorus pesticides. *Anal Chem* **93**, 7275–7282.
6. Duan S, Wu X, Shu Z, Xiao A, Chai B, Pi F, Wang J, Dai H, et al (2023) Curcumin-enhanced MOF electrochemical sensor for sensitive detection of methyl parathion in vegetables and fruits. *Microchem J* **184**, 108182.
7. Vaitsis C, Sourkouni G, Argirusis C (2019) Metal organic frameworks (MOFs) and ultrasound: A review. *Ultrason Sonochem* **52**, 106–119.
8. Katz M, Mondloch J, Otten R, Park J, Nguyen S, Farha O, Hupp J (2014) Simple and compelling biomimetic metal-organic framework catalyst for the degradation of nerve agent simulants. *Angew Chem Int Edit* **53**, 497–501.
9. Qin X, Wang M, Ouc Y, Wang F (2025) Absorption and emission spectral response triggered by dipicolinate in a composite structure of luminescent metal framework and rose bengal dye. *ScienceAsia* **51**, 2025085.
10. Graham F (2025) Daily briefing: Chemistry Nobel for 'super sponge' MOFs. *Nature*.
11. Zheng H, Zeng Y, Chen J, Lin R, Zhuang W, Cao R, Lin Z (2019) Zr-based metal-organic frameworks with intrinsic peroxidase-like activity for ultradeep oxidative desulfurization: mechanism of H_2O_2 decomposition. *Inorg Chem* **58**, 6983–6992.
12. Zhang T, Tang M, Yang S, Fa H, Wang Y, Huo D, Hou C, Yang M (2025) Development of a novel ternary MOF nanozyme-based smartphone-integrated colorimetric and microfluidic paper-based analytical device for trace glyphosate detection. *Food Chem* **464**, 141780.
13. Wu G, Liu S, Du C, Huang M, Wu Y, Shen Y (2024) A versatile visual molecular imprinting-driven switchable nanozyme activity-based trimodal assay and logic gate circuits of ethyl carbamate. *Anal Chem* **96**, 14706–14713.
14. Qi J, Hao W, Li J, Wan Y, Jiang G, Ozaki Y, Pi F (2025) PCN222(Fe)@NU-1000 based MOF-on-MOF dual-signal sensing strategy for sensitive detection of phoxim. *Microchem J* **218**, 115260.
15. Zhou J, Xiong D, Zhang H, Xiao J, Huang R, Qiao Z, Yang Z, Zhang Z (2025) Targeted enrichment of nucleic acid bionic arms enhances the hydrolysis activity of nanozymes for degradation and real-time monitoring of organophosphorus pesticides in water. *Environ Sci Technol* **59**, 1844–1853.
16. Wu G, Du C, Peng C, Qiu Z, Li S, Chen W, Qiu H, Zheng Z, et al (2024) Machine learning-assisted laccase-like activity nanozyme for intelligently onsite real-time and dynamic analysis of pyrethroid pesticides. *J Hazard Mater* **480**, 136015.
17. Nguyen K, Vo N, Le K, Ho K, Phan N, Ho P, Le H (2023) Defect-engineered metal-organic frameworks (MOF-808) towards the improved adsorptive removal of organic dyes and chromium (VI) species from water. *New J Chem* **47**, 6433–6447.
18. Ding J, Guo D, Wang N, Wang H, Yang X, Shen K, Chen L, Li Y (2023) Defect engineered metal-organic framework with accelerated structural transformation for efficient oxygen evolution reaction. *Angew Chem Int Edit* **62**, e202311909.
19. Wu G, Dilinaer A, Nie P, Liu X, Zheng Z, Luo P, Chen W, Wu Y, et al (2023) Dual-modal bimetallic nanozyme-based sensing platform combining colorimetric and photothermal signal cascade catalytic enhancement for detection of hypoxanthine to judge meat freshness. *J Agric Food Chem* **71**, 16381–16390.
20. Wu H, Xu Z, Xiong D, Qin X, Liu G, Zhang H (2023) Two dimensional iron metal-organic framework nanosheet with peroxidase-mimicking activity for colorimetric detection of hypoxanthine related to shrimp freshness. *Talanta* **265**, 124833.
21. Meneses L, Gajardo-Parra N, Cea-Klapp E, Garrido J, Held C, Duarte A, Paiva A (2023) Improving the activity of horseradish peroxidase in betaine-based natural deep eutectic systems. *RSC Sustain* **1**, 886–897.
22. Song D, Zou Y, Tian T, Ma Y, Huang H, Li Y (2024) Machine learning-assisted melamine-Cu nanozyme and cholinesterase integrated array for multi-category pesticide intelligent recognition. *Biosens Bioelectron* **266**, 116747.
23. Li Q, Guo Y, He X, Li G (2023) Bifunctional Cu(II)-containing PDA-PEI copolymer dots: demonstration of a dual-mode platform for colorimetric-fluorescent detection of glyphosate in the environment. *Talanta* **265**, 124865.
24. Li F, Jiang J, Peng H, Li C, Li B, He J (2022) Platinum nanozyme catalyzed multichannel colorimetric sensor array for identification and detection of pesticides. *Sens Actuators B Chem* **369**, 132334.
25. Shi W, Li T, Chu N, Liu X, He M, Bui B, Chen M, Chen W (2021) Nano-octahedral bimetallic Fe/Eu-MOF preparation and dual model sensing of serum alkaline phosphatase (ALP) based on its peroxidase-like property and fluorescence. *Mater Sci Eng C-Mater Biol Appl* **129**, 112404.
26. Li M, Zhang S, Li H, Chen M (2023) Cerium/polyacrylic acid modified porphyrin metal-organic framework as fluorescence and photothermal sensor for ascorbic acid measurement. *Talanta* **252**, 123825.
27. Rocha L, Steiner B, Prado Cechinel M, Riella H, Padoin N, Soares C (2025) Green synthesis of *Pereskia aculeata*-based carbon dots toward qualitative glyphosate detection. *Chem Eng Sci* **316**, 121986.
28. Yadav P, Zelder F (2021) Detection of glyphosate with a copper(II)-pyrocatechol violet based GlyPKit. *Anal Methods* **13**, 4354–4360.
29. Dong J, Hu Y, Su X, Yao Y, Zhou Q, Gao M (2024) Low-background interference detection of glyphosate, glufosinate, and AMPA in foods using UPLC-MS/MS without derivatization. *Anal Bioanal Chem* **416**, 1561–1570.
30. Aydin Z, Keleş M (2022) A reaction-based system for the colorimetric detection of glyphosate in real samples. *Spectrochim Acta A Mol Biomol Spectrosc* **267**, 120501.
31. He J, Zhang L, Chu F, Miao F, Tao B, Zang Y (2022) Fabrication of a composite electrode applied in photoelectrochemical detection of glyphosate. *Vacuum* **205**, 111428.

Appendix A. Supplementary data

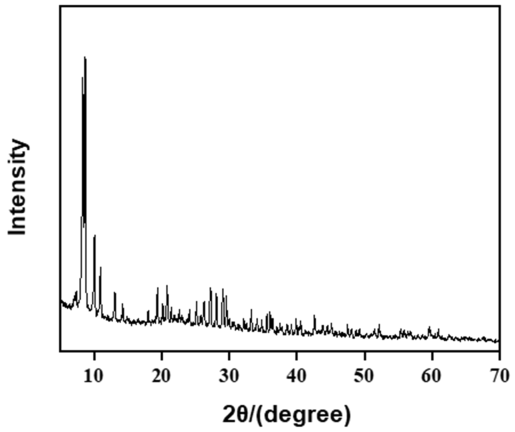

Fig. S1 XRD spectrum of MOF-808-NH_2.

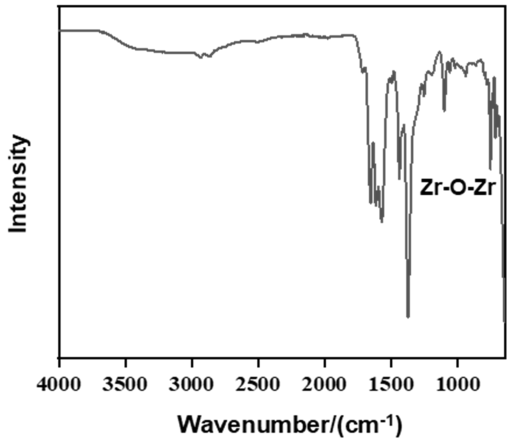

Fig. S2 FT-IR spectrum of MOF-808-NH_2.

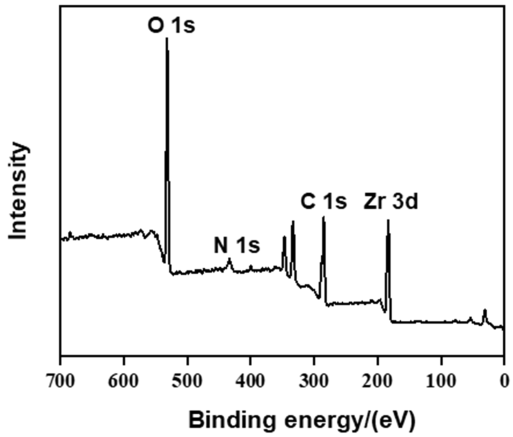

Fig. S3 XPS spectrum of MOF-808-NH_2.

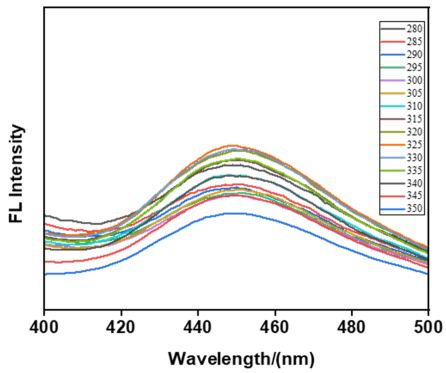

Fig. S4 Fluorescence spectra of MOF-808-NH_2 under different excitations.

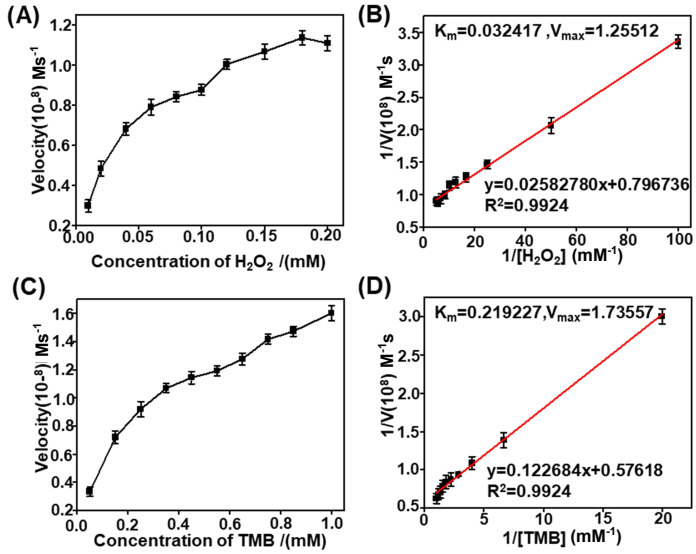

Fig. S5 (A,B) The steady-state kinetics and the corresponding double-reciprocal plot of MOF-808-NH_2 toward H_2O_2, at a fixed H_2O_2 concentration (200 μM) and varying TMB concentrations. (C,D) The steady-state kinetics and the corresponding double-reciprocal plot of MOF-808-NH_2 toward TMB at a fixed TMB concentration (1 nM) and varying H_2O_2 concentrations. Experimental conditions: MOF-808-NH_2, 50 μg/ml; HAc–NaAc buffer (pH 4); 25 min; 45 °C.

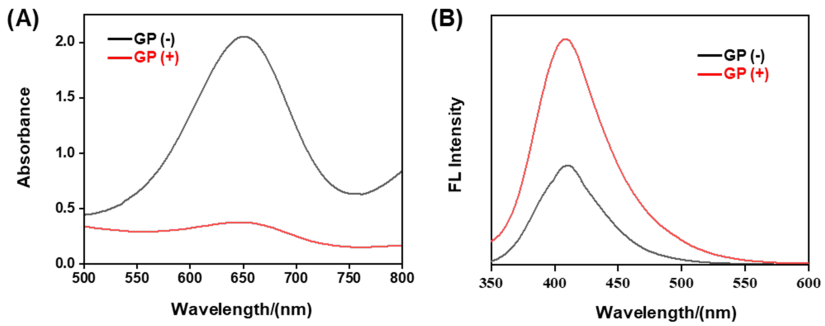

Fig. S6 (A) Absorption and (B) fluorescence spectra under 325 nm excitation of MOF-808-NH_2 + H_2O_2 + TMB (-) without and (+) with GP.